

Structure of Dark Matter Halos in Cosmological Simulations

Alan R. Duffy^{1,2}, Joop Schaye², Scott T. Kay¹ and Claudio Dalla Vecchia²

¹*Jodrell Bank Centre for Astrophysics, Alan Turing Building, University of Manchester, M13 9PL, U.K.*

²*Leiden Observatory, Leiden University, PO Box 9513, 2300 RA Leiden, The Netherlands*

We have used three large N -body simulations to investigate the dependence of dark matter halo concentrations on halo mass and redshift in the WMAP year 3 cosmology. The median concentration - mass relation is well fit by a power law over the mass range $10^{11} - 10^{15} h^{-1} M_{\odot}$ at redshifts $z < 2$, for both NFW and Einasto density profiles. We compare our findings to recent work based on the **Millennium Simulation**, which uses a higher value of σ_8 , consistent with the WMAP year 1 cosmology. We find that for $z = 0$, halo concentrations are reduced by up to 34 per cent at $10^{11} h^{-1} M_{\odot}$, and 19 per cent at $10^{14} h^{-1} M_{\odot}$.

1 Introduction

It has been argued¹ that the concentration of a halo reflects the background density of the Universe at its formation time, and as small objects form first in a hierarchical universe, lower mass halos will be more concentrated than massive ones.

We have used three DM only simulations, run with GADGET2². Each simulation contains 512^3 DM particles but with a progressively larger comoving box size: 25, 100, and $400 h^{-1} \text{Mpc}$ for runs *L025*, *L100* and *L400*, respectively. We have used the 3 year Wilkinson Microwave Anisotropy Probe (WMAP) cosmology⁶, hereafter WMAP3, and compared with the **Millennium Simulation**⁴ (MS) $c(M)$ relation⁵ for the first year WMAP release⁷ henceforth WMAP1; where σ_8 is about 23 per cent larger, therefore one can expect a given mass halo to form at earlier times and hence with higher concentration. Please refer to Duffy *et al*³ for further details.

1.1 Density Profiles

The Navarro-Frenk-White¹ (NFW) density profile is given by

$$\rho(r) = \rho_{\text{crit}} \frac{\delta_c}{(r/r_s)(1+r/r_s)^2}, \quad (1)$$

where δ_c is a characteristic density contrast and r_s is a scale radius. The concentration parameter is defined as $c_{200} \equiv r_{200}/r_s$. NFW profiles were fit using the two parameters r_s and δ_c . Other concentrations, e.g. c_{vir} and c_{mean} , can also be defined for different overdensity values.

The Einasto profile is a rolling power-law first introduced to describe the distribution of old stars in the Milky Way⁸. It takes the form

$$\ln(\rho/\rho_{-2}) = -\frac{2}{\alpha} [(r/r_{-2})^\alpha - 1], \quad (2)$$

where ρ_{-2} is the density at r_{-2} the radius where $\frac{d \ln \rho}{d \ln r} = -2$ and α is the rate at which the profile turns over. An analagous concentration to the NFW case can be defined using r_{-2} .

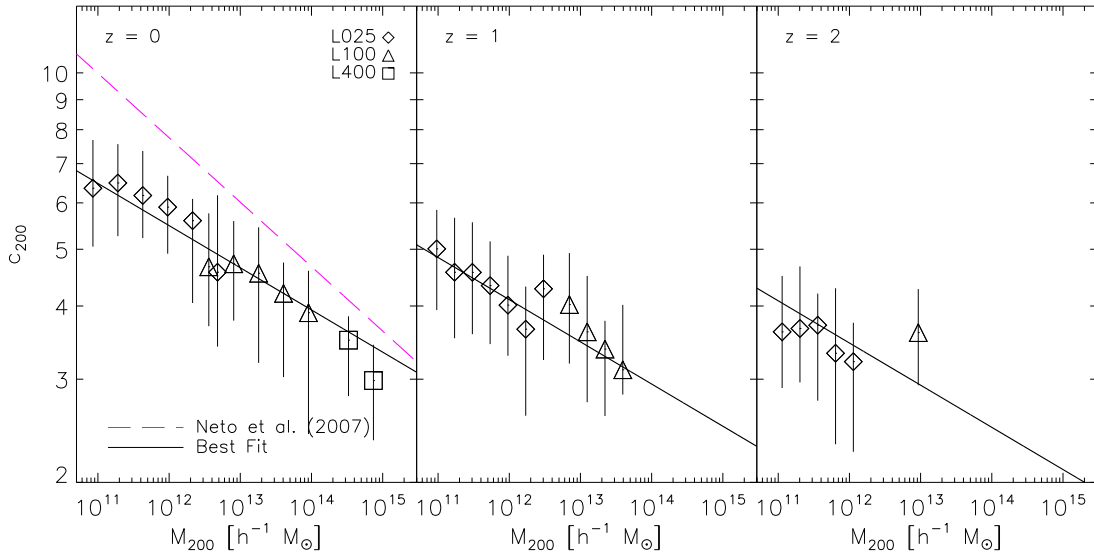


Figure 1: Concentration-mass relations for $z = 0$ (top), 1 (middle) and 2 (bottom) using NFW density profiles. Data points correspond to median values and error bars to quartiles. Only bins containing at least 5 haloes are shown. The solid lines show the best-fit power-law relation. The errors on the best-fit parameters, given in the legend, are determined by bootstrap sampling the haloes and correspond to 68.2 per cent confidence limits. The dashed line in the left panel shows the best-fit power-law relation from Neto *et al.*

Table 1: Best-fit parameters for the median $c(M, z)$ relation using $M_{\text{pivot}} = 2 \times 10^{12} h^{-1} M_{\odot}$ for three halo definitions using two different density profiles. The errors correspond to 1σ confidence intervals and have been determined by bootstrap resampling the halos.

Overdensity	NFW			Einasto		
	A	B	C	A	B	C
c_{200}	$5.22 \pm_{0.15}^{0.13}$	$-0.072 \pm_{0.009}^{0.009}$	$-0.42 \pm_{0.05}^{0.05}$	$5.70 \pm_{0.19}^{0.18}$	$-0.092 \pm_{0.010}^{0.009}$	$-0.55 \pm_{0.06}^{0.06}$
c_{vir}	$7.28 \pm_{0.21}^{0.19}$	$-0.075 \pm_{0.009}^{0.009}$	$-0.69 \pm_{0.05}^{0.06}$	$8.05 \pm_{0.27}^{0.24}$	$-0.100 \pm_{0.009}^{0.009}$	$-0.85 \pm_{0.06}^{0.06}$
c_{mean}	$9.61 \pm_{0.28}^{0.25}$	$-0.073 \pm_{0.009}^{0.009}$	$-1.01 \pm_{0.06}^{0.06}$	$10.62 \pm_{0.35}^{0.31}$	$-0.098 \pm_{0.009}^{0.009}$	$-1.16 \pm_{0.06}^{0.06}$

2 Results

The data, which spans four orders of magnitude in mass and a redshift range $z = 0 - 2$ are well described by a function of the form

$$c = A(M/M_{\text{pivot}})^B(1+z)^C. \quad (3)$$

The parameter values and errors are given in Table 1.

References

1. Navarro, J., Frenk, C., & White, S., 1997, ApJ, 490, 493
2. Springel, V., 2005, MNRAS, 364, 1105
3. Duffy, A., Schaye, J., Kay, S., T., Dalla Vecchia, C., 2008, arXiv:0804.2486
4. Springel, V., White, S., Jenkins, A., et al., 2005, Nature, 435, 629
5. Neto, A., Gao, L., Bett, P., Cole S., Navarro J.F., Frenk C.S., White S.D.M., Springel V., 2007, MNRAS, 381, 1450
6. Spergel, D. N., Bean, R., Dofé, O., et al., 2007, ApJ, 170, 377s
7. Spergel, D., Verde, L., Peiris, H., et al., 2003, ApJS, 148, 175
8. Einasto, J., 1965, Alma-Ata, 51, 87